

# Inverse problem for extragalactic transport of ultra-high energy cosmic rays

V.S. Ptuskin S.I. Rogovaya and V.N. Zirakashvili

Pushkov Institute of Terrestrial Magnetism, Ionosphere and Radio Wave Propagation of the Russian Academy of Sciences (IZMIRAN),  
Troitsk, Moscow 142190, Russia

E-mail: [vptuskin@izmiran.ru](mailto:vptuskin@izmiran.ru), [rogovaya@izmiran.ru](mailto:rogovaya@izmiran.ru), [zirak@izmiran.ru](mailto:zirak@izmiran.ru)

**Abstract.** The energy spectra and composition of ultra-high energy cosmic rays are changing in a course of propagation in the expanding Universe filled with background radiation. We developed a numerical code for solution of inverse problem for cosmic-ray transport equations that allows the determination of average source spectra of different nuclei from the cosmic ray spectra observed at the Earth. Employing this approach, the injection spectra of protons and Iron nuclei in extragalactic sources are found assuming that only these species are accelerated at the source. The data from the Auger experiment and the combined data from the Telescope Array + HiRes experiments are used to illustrate the method.

---

## Contents

<b>1</b>	<b>Introduction</b>	<b>1</b>
<b>2</b>	<b>Solution of inverse problem for a system of cosmic-ray transport equations</b>	<b>2</b>
<b>3</b>	<b>Approximation of experimental data</b>	<b>4</b>
<b>4</b>	<b>Results of Calculations</b>	<b>5</b>
<b>5</b>	<b>The use of the measured mean logarithm of <math>A</math></b>	<b>6</b>
<b>6</b>	<b>Discussion and Conclusion</b>	<b>9</b>

---

## 1 Introduction

The origin of cosmic rays with energies  $E > 10^{18}$  eV remains a key problem of cosmic ray astrophysics. The observed suppression of cosmic ray flux at energies above  $\sim 5 \times 10^{19}$  eV seems confirm the presence of the GZK cutoff predicted in [1, 2] although the suppression due to the acceleration limits in cosmic ray sources can not be excluded [3, 4]. The occurrence of the GZK suppression and the high isotropy of the highest energy cosmic rays are indicative of their extragalactic origin. The list of potential sources which could give the observed cosmic ray flux includes active galactic nuclei, gamma-ray bursts, fast spinning newborn pulsars, interacting galaxies, large-scale structure formation shocks and some other objects, see reviews [5–7] and references therein.

The present knowledge about the highest energy cosmic rays was mainly acquired from the High Resolution Fly’s Eye Experiment (HiRes), Pierre Auger Observatory (Auger), Telescope Array experiment (TA), and from the Yakutsk complex EAS array, see [5, 8, 9]. The mass composition of these cosmic rays remains uncertain. The interpretation of HiRes and TA data favors predominantly proton composition at energies  $10^{18}$  to  $5 \times 10^{19}$  eV, whereas the Auger data indicate that the cosmic ray composition is becoming heavier with energies changing from predominantly proton at  $10^{18}$  eV to more heavy and approaching Iron composition at about  $5 \times 10^{19}$  eV. The mass composition interpretation of the measured quantities depends on the assumed hadronic model of particle interactions which is based on not well determined extrapolation of physics from lower energies.

The energy spectrum in extragalactic sources is commonly determined by the trial-and-error method when one makes the calculations of the expected at the Earth cosmic ray intensity assuming some shape of the source energy spectrum and the source composition. The calculations follow cosmic ray propagation from the source to the observer, e. g. [10]. The standard assumption is that the source spectrum is a power law on magnetic rigidity up to some maximum rigidity.

In the present work we show how to inverse the procedure and calculate the source function starting from the observed at the Earth spectrum without ad hoc assumptions about the shape of source spectrum. Simple cases of the source composition that includes protons and Iron nuclei are considered and the analytical approximations of the data from Auger and TA+HiRes experiments are used.

## 2 Solution of inverse problem for a system of cosmic-ray transport equations

We use the following transport equation for cosmic ray protons and nuclei in the expanding Universe filled with the background electromagnetic radiation (see [11] for details):

$$\begin{aligned}
 & -H(z)(1+z)\frac{\partial}{\partial z}\left(\frac{F(A,\varepsilon,z)}{(1+z)^3}\right) - \\
 & -\frac{\partial}{\partial\varepsilon}\left(\varepsilon\left(\frac{H(z)}{(1+z)^3} + \frac{1}{\tau(A,\varepsilon,z)}\right)F(A,\varepsilon,z)\right) + \nu(A,\varepsilon,z)F(A,\varepsilon,z) \\
 & = \sum_{i=1,2,\dots} \nu(A+i \rightarrow A,\varepsilon,z)F(A+i,\varepsilon,z) + q(A,\varepsilon)(1+z)^m. \tag{2.1}
 \end{aligned}$$

The system of eqs. (2.1) for all kinds of nuclei with different mass numbers  $A$  from Iron to Hydrogen should be solved simultaneously. The energy per nucleon  $\varepsilon = E/A$  is used here because it is approximately conserved in a process of nuclear photodisintegration,  $F(A,\varepsilon,z)$  is the corresponding cosmic-ray distribution function,  $z$  is the redshift,  $q(A,\varepsilon)$  is the density of cosmic-ray sources at the present epoch  $z = 0$ ,  $m$  characterizes the source evolution (the evolution is absent for  $m = 0$ ),  $\tau(A,\varepsilon,z)$  is the characteristic time of energy loss by the production of  $e^-e^+$  pairs and pions,  $\nu(A,\varepsilon,z)$  is the frequency of nuclear photodisintegration, the sum in the right side of eq. (2.1) describes the contribution of secondary nuclei produced by the photodisintegration of heavier nuclei,  $H(z) = H_0((1+z)^3\Omega_m + \Omega_\Lambda)^{1/2}$  is the Hubble parameter in a flat universe with the matter density  $\Omega_m (= 0.3)$  and the  $\Lambda$ -term  $\Omega_\Lambda (= 0.7)$ .

The numerical solution of cosmic-ray transport equations follows the finite differences method. The variables are the redshift  $z$  and  $\log(E/A)$ . The maximum value  $z_{max} = 3$  is assumed in our calculations.

A comprehensive analysis of cosmic ray propagation in the intergalactic space was presented in [12].

Equations 2.1 are valid for an arbitrary regime of cosmic ray propagation - diffusion, rectilinear motion, or any intermediate regime. It should be emphasized that an alternative Monte Carlo techniques were used for treating the propagation and interactions of ultra-high energy cosmic rays. A representative list of references was given in [13]. Although more sophisticated, the Monte Carlo method is in general more time consuming compared to the solution of equations 2.1 by the finite differences method.

The assumption of continuous source distribution is not valid when particles lose energy at a scale less than the distance between cosmic ray sources. According to the latest Auger results, the low bound on cosmic ray sources density is estimated as  $n_s \geq (0.06 - 5) \times 10^{-4} \text{Mpc}^{-3}$ , [14]. The finite distance to the nearest source is approximately taken into account in our calculations by the cutoff of the source distribution at  $z_{min} \approx 0.48H_0d/c \ll 1$ , so that  $q = 0$  at  $z \leq z_{min}$  ( $0.48d$  is the average distance of an observer to the nearest source if point sources arrange a cubic lattice with the edge, the distance between sources, equals to  $d$ ). The statistically uniform source distribution is assumed at larger redshifts.

The stochastic nature of interactions is not taken into account in our transport equations. The Monte Carlo modelling that includes this effect and the analytical model, which is a simplified version of the model used in our calculations, were compared in [15]. A fairly good agreement of both calculated spatial distributions of secondary species produced by an isolated source of ultra high-energy cosmic rays was found. A similar conclusion was made in the work

[16]. The difference for the Iron source is less than 15 percent that satisfies the needs of our work. The ultra-high energy proton spectrum is affected by fluctuations in the photopion production. The noticeable effect of fluctuations is expected at energies  $E \geq 1 \times 10^{20}$  eV. The Monte Carlo simulations of the proton propagation at  $n_s = 10^{-5} \text{Mpc}^{-3}$  [17] showed not more than  $\sim 10$  percent difference at  $E > 6 \times 10^{19}$  eV compared to the calculations made in the model with continuous energy loss and the homogeneous source distribution. These results characterize the errors in our approximations of cosmic ray transport process.

Let us introduce solution  $G(A, \varepsilon; A_s, \varepsilon_s)$  of eqs. (2.1) at  $z = 0$  for a delta-source  $q(A, \varepsilon) = \delta_{AA_s} \delta(\varepsilon - \varepsilon_s)$ . This source function describes the emission of nuclei with mass number  $A_s$  and energy  $\varepsilon_s$  from cosmic ray sources distributed over all  $z$  up to  $z_{\text{max}}$ . The general solution of eqs. (2.1) at the observer location  $z = 0$  can now be presented as

$$F(A, \varepsilon, z = 0) = \sum_{A'} \int d\varepsilon' G(A, \varepsilon; A', \varepsilon') q(A', \varepsilon'),$$

$$N(A, E, z = 0) = A^{-1} \sum_{A'} \int d\varepsilon' G(A, E/A; A', \varepsilon') q(A', \varepsilon') \quad (2.2)$$

Here  $N(A, E, z)$  is the spectrum of nuclei with atomic mass  $A$  as the function of the total energy  $E$ . The observed all-particle spectrum is determined by the summation over all types of nuclei  $\sum_A N(A, E, z = 0)$ .

The set of discrete values of particle energies  $E_i$  and  $\varepsilon_i$  is defined to solve the transport equation numerically. The grid with constant  $\Delta\varepsilon/\varepsilon$  and with 100 energy bins per decade is used in our calculations. Eq. (2.2) in the discrete form is

$$N_i(A, z = 0) = A^{-1} \sum_{j, A'} (\Delta\varepsilon)_j G_{ij}(A; A') q_j(A'), \quad (2.3)$$

where the subscript indexes  $i$  and  $j$  denote the corresponding energies  $E_i$  and  $\varepsilon_j$ . The all particle spectrum is  $\sum_A N_i(A, z = 0)$ .

The source term  $q_j(A)$  for each type of nuclei can be derived from the system of linear eqs. (2.3) if the observed spectra  $N_i(A, z = 0)$  for all types of nuclei are known. In fact, the detailed information on the spectra of individual types of nuclei  $N_i(A, z = 0)$  is usually not available.

If only the all particle spectrum  $\sum_A N_i(A, z = 0)$  is known, the source spectra can be found when the source abundances for different types of ions are specified. In the simplest case, when only nuclei with mass number  $A = A_s$  are accelerated in the sources, eq. (2.3) allows to find the following relation:

$$q_j(A_s) = \sum_i \left( \sum_A A^{-1} (\Delta\varepsilon)_j G_{ij}(A, A_s) \right)^{-1} \times \sum_A N_i(A, z = 0). \quad (2.4)$$

In another physically justified case, the source terms for all primary nuclei are similar functions of magnetic rigidity  $R = E/Z$ , so that  $q(A, \varepsilon) = S_A Q(A\varepsilon/Z)$  where  $S_A$  are the normalization coefficients. The last equation in a matrix form can be presented as

$$q_j(A') = \sum_k M_{jk}(A') Q_k, \quad (2.5)$$

where  $\mathbf{M}$  is a matrix, which provides the needed dependence of the source term on rigidity. The relation  $Z = A/2$  is assumed in our calculations for all nuclei heavier than protons.

The formal solution of the inverse problem is now

$$Q_k = \sum_i \left( \sum_{A, A', j} A^{-1} (\Delta \varepsilon)_j G_{ij}(A, A') M_{jk}(A') \right)^{-1} \times \sum_A N_i(A, z=0). \quad (2.6)$$

Technically, the calculations of inverse matrixes in eqs. (2.4, 2.6) are straightforward since  $G_{ij}$  is the triangular matrix owing to the monotonic decrease of particle energy in a course of its transport in the intergalactic medium. However, as it is known from the analysis of equations of such kind [18], the solutions of the integral and matrix eqs. (2.2, 2.3) do not depend continuously on their right-hand sides. The small errors in the data  $N(A, E, z=0)$  may be greatly amplified in the solution  $q(A, \varepsilon)$ , so that the inverse problem is ill-posed. In essence, the difficulty posed by inverse problems is that we are obliged to work not with exact  $N(A, E, z=0)$  but with its estimate obtained by measurements and therefore subject to accidental errors. Additional errors occur because of the approximate description of cosmic ray propagation. Different regularization procedures can be used to deal with these problems [18–20]. Below we try to work in the region of parameters where the regularization is not required. In particular, the consideration is limited to not more than two types of nuclei in the sources, the protons and Iron, and the Iron-to-proton source ratio is not too low that alleviates the problem.

### 3 Approximation of experimental data

To simplify calculations and damp the spread of data points in the measured at the Earth cosmic ray spectrum, we use its analytical approximations.

The combined results of the TA and HiRes measurements [21] are presented in figure 1, where the straight lines show the approximation suggested in [21]. Based on this approximation, we use the following formula for the observed at the Earth spectrum in our calculations:

$$\begin{aligned} J &\propto E^{-3.283}, E < 5.04 \times 10^{18} \text{eV}; \\ J &\propto E^{-2.685} \times [1 + (E/(5.8 \times 10^{19} \text{eV}))^{1.935} \times \\ &\exp(-(7 \times 10^{19} \text{eV}/E)^2)]^{-1}, E > 5.04 \times 10^{18} \text{eV}. \end{aligned} \quad (3.1)$$

The corresponding approximation of the TA+HiRes data is shown by the dash gray line in figure 1.

The formula

$$\begin{aligned} J(E) &\propto E^{-3.23}, E < 5 \times 10^{18} \text{eV}; \\ J(E) &\propto E^{-2.63} \times [1 + \exp(\log(E/10^{19.63} \text{eV})/0.15)]^{-1} \times \\ &\exp(-(E/(1.5 \times 10^{20} \text{eV}))^4), E > 5 \times 10^{18} \text{eV}. \end{aligned} \quad (3.2)$$

is used in our calculations to approximate the Auger data [22], see figure 2. This formula is similar to the equation suggested by the Auger team but contains  $\exp(-(E/1.5 \times 10^{20} \text{eV})^4)$  factor of cosmic ray flux suppression at energies  $\gtrsim 1.5 \times 10^{20}$  eV.

Using the Auger data on energy dependence of the mean logarithm of the atomic mass number  $\langle \ln A \rangle$  calculated in the EPOS-LHC model of particle interactions in the atmosphere [22], we accept the following approximation

$$\langle \ln A \rangle = 0.5 + 4.2 \times (E/10^{20} \text{eV})^{0.6} \quad (3.3)$$

shown by the dash line in figure 7 below.

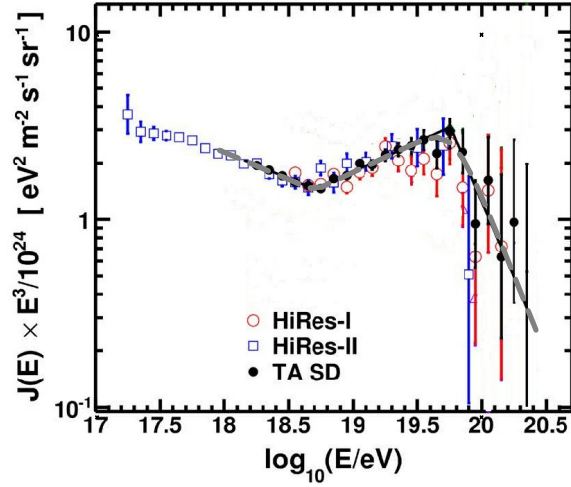


**Figure 1.** Analytical approximations used in the present calculations to describe TA+HiRes data are shown by dash gray line together with the experimental data and its straight-line approximation (thin black lines) [21].

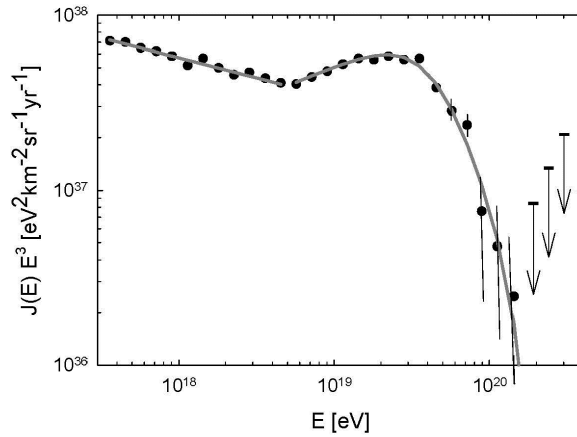


**Figure 2.** Analytical approximations used in the present calculations to describe the Auger data are shown by solid line together with Auger data [22].

## 4 Results of Calculations

We first make calculations of the source spectra in two simple cases of pure proton and pure Iron source composition. The results are shown in figures 3 for the Auger data and 4 for the

TA+HiRes data. The dark lines refer to a pure proton source and the gray lines refer to a pure Iron source. The solid lines illustrate the case without source evolution  $m = 0$  (as it can be if the sources are the BL Lacs type galaxies, see [12]); the dash lines describe the case of AGN with a strong evolution where  $m = 3.2$  at  $z < 1.2$  and the evolution is saturated at larger  $z$  [23]. It is clear from figures 3 and 4 that the strong cosmological evolution leads to the decrease of required source power at low cosmic ray energies. The difference with the source spectrum without evolution reaches the factor of about 4 at  $10^{18}$  eV. The dotted lines show the results of calculations with a non-zero distance to the nearest source  $z_{min} \neq 0$  at the source number density  $n_s = 10^{-4}$  Mpc $^{-3}$ . It is clear that the finite distance to the nearest source requires the increase of source power at the highest energies of accelerated particles. The power law asymptotic behavior of the TA+HiRes cosmic ray spectrum (3.1) at the highest energies can not be reproduced for the pure Iron source at  $n_s = 10^{-4}$  Mpc $^{-3}$ .

The kinks in all source spectra at about  $5 \times 10^{18}$  eV are due to the corresponding discontinuities of the first derivatives of the expressions (3.1) and (3.2) and in this sense they are artificial. The power law tail at the highest energies in eq. (3.1) describing the observed spectrum results in the extension of the calculated TA+HiRes source spectra to higher energies compared to the calculated Auger source spectra. The difference between these two experiments is much smaller at energies below  $(3..5) \times 10^{19}$  eV where the data are more accurate. The difference between proton and Iron sources at these relatively low energies is evident: the proton source spectrum can be better approximated by a power law compared to the concave Iron spectrum. It is explained by the influence of energy loss on the  $e^-e^+$  production in the case of ultra high energy protons moving through the background radiation [12]. After propagation in the intergalactic space, this process produces the characteristic dip in the initial power law proton spectrum at around  $5 \times 10^{18}$  eV while the Iron nuclei preserve the shape of their source spectrum.

The results of calculations when both proton and Iron are present in the source and their spectra are similar functions of magnetic rigidity are shown in figure 5. One can see how the results of calculations depend on the assumed Iron-to-proton source ratio  $S_{Fe}/S_p$ .

The calculated elemental composition of cosmic rays at the Earth for the case  $S_{Fe}/S_p = 10^{-2}$  is presented in figure 6. The corresponding value of  $\langle \ln(A) \rangle$  is shown in figure 7. It is evident that our very simple model with only two primary species at the source (protons and Iron nuclei), does not reproduce the observed  $\langle \ln A \rangle$  except the energies  $\sim 10^{18}$  eV where the protons and light nuclei dominate and the highest energies where the Iron group nuclei dominate. The intermediate nuclei are certainly needed at the source to reproduce observations at all energies.

## 5 The use of the measured mean logarithm of $A$

The source spectra of protons and Iron can be found if the measurements of the mean logarithm  $\langle \ln A \rangle$  are available in addition to the all-particle spectrum. Then using Eq. (2.3) one has the following two systems of equations for  $q_j(1)$  and  $q_j(56)$ :

$$\sum_A N_i(A, z=0) = \sum_{A,j} (\Delta\varepsilon)_j (G_{ij}(A; 1)q_j(1) + 56^{-1}G_{ij}(A; 56)q_j(56)), \quad (5.1)$$

$$\langle \ln A \rangle_i \sum_A N_i(A, z=0) = \sum_{A,j} (\Delta\varepsilon)_j G_{ij}(A; 56) \frac{\ln(A)}{A} q_j(56), \quad (5.2)$$

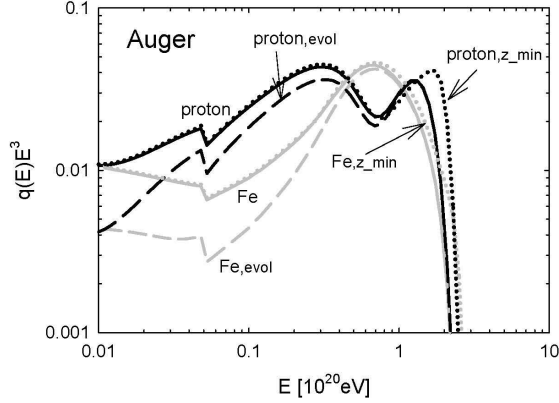


**Figure 3.** Calculated source spectra in arbitrary units based on the approximated analytically Auger data. Black lines for proton source; gray lines for Iron source. Solid lines correspond to the homogeneous source distribution without evolution,  $m = 0$ . Dotted lines correspond to the spatial source distribution with a finite distance to the nearest source located at the redshift  $z_{min} = 0.0024$  at  $m = 0$ . Dash lines are the source spectra for homogeneous source distribution with evolution described in the text.

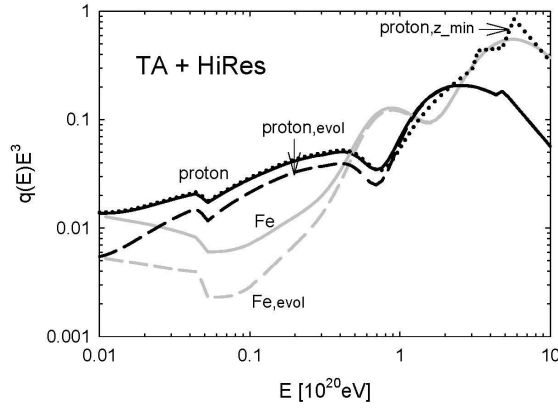


**Figure 4.** The same as figure 3 but for the approximated analytically TA+HiRes data.

The source spectrum of Iron  $q_j(56)$  is found from the last system of equations. After that the source spectrum of protons  $q_j(1)$  is obtained solving the system of equations (5.1).

As a result both the observed all particle cosmic-ray Auger spectrum at the Earth approximated by eq. (3.2) and the  $\langle \ln A(E) \rangle$  given by eq. (3.3) can be exactly reproduced assuming that only protons and Iron nuclei are present in the source. The corresponding



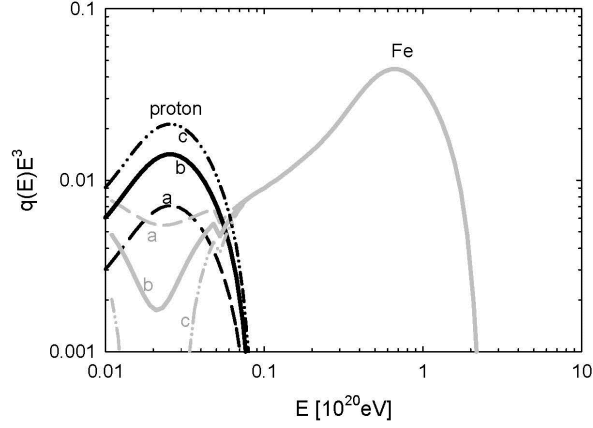


**Figure 5.** Calculated source spectra based on the Auger data for different Iron-to-proton source ratios indicated by (a) for  $S_{Fe}/S_p = 2 \times 10^{-2}$ , (b) for  $S_{Fe}/S_p = 10^{-2}$ , and (c) for  $S_{Fe}/S_p = 6.7 \times 10^{-3}$ . Black lines for proton source; gray lines for Iron source. Proton and Iron source spectra have the same dependence on magnetic rigidity. Homogeneous source distribution without evolution is assumed.

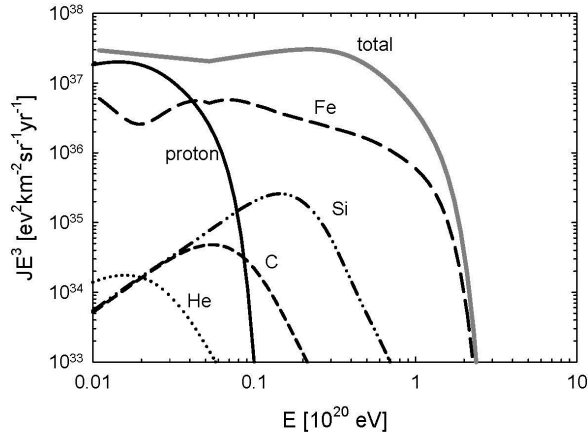


**Figure 6.** Calculated spectra of different types of nuclei for Iron-to-proton source ratio  $S_{Fe}/S_p = 10^{-2}$  and the total Auger cosmic ray spectrum at the Earth.

calculated source spectra are shown in figure 8. They have different dependence on magnetic rigidity.

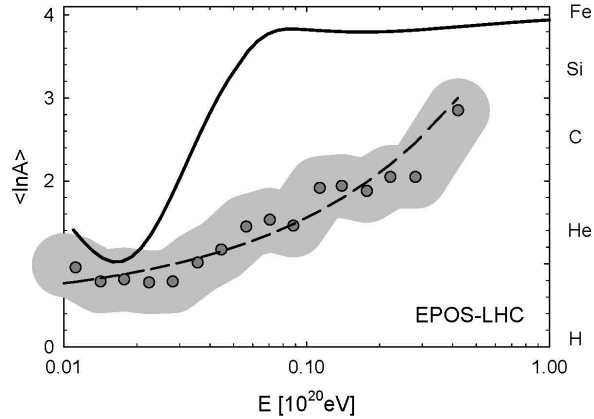


**Figure 7.** Calculated value of  $\langle \ln A \rangle$  (solid line) together with corresponding Auger data (dots and gray regions which characterizes errors in determination of  $\langle \ln A \rangle$  in the EPOS LHC interaction model). Dash line shows our approximation (3.3).

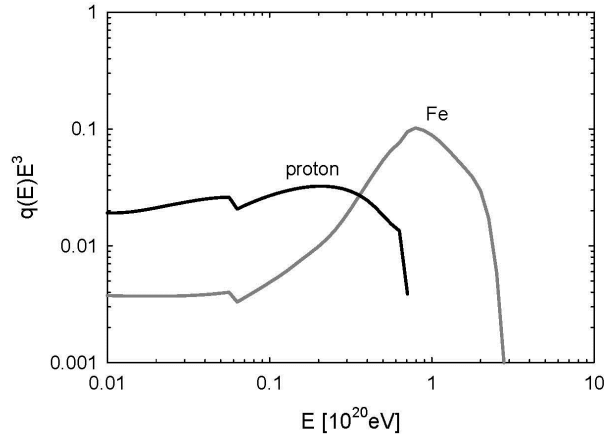


**Figure 8.** Calculated source spectra of protons and Iron based on Auger data on cosmic ray spectrum and  $\langle \ln A \rangle$ . Homogeneous source distribution without evolution is assumed.

## 6 Discussion and Conclusion

We showed how one can find average spectrum of extragalactic sources from the cosmic ray spectrum observed at the Earth. This task was formulated as an inverse problem for the system of transport eqs. (2.1) that describe the propagation of ultra-high energy cosmic rays in the expanding Universe filled with the background electromagnetic radiation.

The purpose of the present paper was the demonstration of general approach to the prob-

lem. The simple settings were considered. The two variants of observed cosmic ray spectrum were used in the calculations. One was taken from the Auger data [22] and approximated by formula (3.2). The other presented the combined TA+HiRes data [21] approximated by eq. (3.1). It was assumed that only two kinds of nuclei (proton and Iron) were present in the sources and the cases of a pure proton, pure Iron, and the mixed source composition were considered. In the last case the calculations were made for the following two scenarios: 1) the proton and Iron source spectra have the same shape on rigidity; 2) the source spectra and the Iron-to-proton ratio are forced to reproduce the observed at the Earth value of  $\langle \ln A \rangle$ . Mathematically, the inverse problems for transport equations (2.1) are ill-posed in the general case that manifests itself in the instability of derived solutions. It explains to a large extent simple assumptions used in the present paper. We plan specifically study this problem in a future publication.

Two additional factors that may impact on the interpretation of the derived source spectra at energies close to  $10^{18}$  eV is worth to mention. The first is the possible contribution of the Galactic sources that may dominate in the observed cosmic ray spectrum at  $< 3 \times 10^{18}$  eV, see e.g. [12] for discussion. The second is the strong deflection of cosmic ray trajectories in magnetic field that may produce the so called magnetic horizon effect in the expanding Universe. It is essential for the wide range of magnetic fields 0.1–10 nG and distances between sources  $d \geq 50$  Mpc at particle energies  $E < 10^{18} Z$  eV [24]. The particle transmission factor at various distances to the source as a function of particle energy was calculated in [25]. This factor characterises the suppression of cosmic ray intensity due to the magnetic horizon effect. Using results of these calculations and assuming that the value of the intergalactic magnetic field is 1 nG and its correlation length is 1 Mpc, one can find that the magnetic horizon effect is not significant for Iron nuclei with energies above  $10^{18}$  eV if cosmic ray source density is not smaller than  $\sim 10^{-4} \text{Mpc}^{-3}$ . It is in the limits of the low bound on cosmic ray sources density found at the GZK energies in the Auger experiment [14]. It should be pointed out that the source density may increase with the decreasing of energy of accelerated particles. For example, such a behavior was found in the model of cosmic ray acceleration by the AGN jets with the observed distribution on kinetic energy where more numerous weak jets contribute most to small cosmic ray energies [11]. The experimental indication of this effect was found in [26]. The calculations of the source spectra in the present paper ignored the presence of the intergalactic magnetic field. It means that the found source spectra may contain depending on magnetic rigidity transmission factor that should be calculated independently assuming some magnetic field properties and the cosmic ray source distribution.

It is difficult to make firm astrophysical statements about cosmic ray source spectra and composition from our simple modelling. However, some conclusions can be made. Recall that the kinks in the calculated source spectra at about  $5 \times 10^{18}$  eV reflect the corresponding discontinuities in the derivatives of the approximation eqs. (3.1, 3.2) and are artificial in this sense. To demonstrate the specific character of the inverse problem solutions, we did not correct the unphysical approximations of the observed spectra.

Accepting that the TA+HiRes data favour the proton source, one can see from figure 4 that the source spectrum at  $m = 0$  is close to the power law  $\propto E^{-2.6}$  below  $\sim 4 \times 10^{19}$  eV with some deviations above this energy and bending down at  $\gtrsim 5 \times 10^{20}$  eV. Notice that statistics above  $3 \times 10^{19}$  eV is poor and the power law approximation of data (3.1) is not very reliable at the highest energies. The proton source spectrum  $E^{-2.55}$  to  $E^{-2.75}$  was derived in the solution of direct transport problem under the assumption of a power-law source spectrum without cosmological source evolution [12].

The Auger data favor the transition from a proton source composition to the Iron one as the energy is rising. With our simple two-species composition, this case is most closely reproduced by the calculations illustrated in figure 5. The obtained source spectra resemble the results [27, 28] based on the analysis of direct transport problems with a power law source spectrum. The maximum magnetic rigidity of accelerated particles  $(3...5) \times 10^{18}$  eV is relatively low in this case that alleviates the problem of cosmic ray acceleration to the extremely high energies. The calculated composition of cosmic rays at the Earth shown in figure 7 considerably deviates from the Auger measurements and certainly requires incorporation of the intermediate nuclei between protons and Iron in the source composition.

The study of inverse transport problem is a useful tool for the investigation of ultra high energy cosmic rays allowing the abandonment of the standard assumption of power law source spectrum with an abrupt cutoff at some maximum magnetic rigidity as it is usually assumed when the direct problem is considered. The present work is a simple illustration of this new approach.

## Acknowledgments

We thank Anatoly Lagutin for useful remarks. The work was supported by the Russian Foundation for Basic Research grant 13-02-00056 and by the Russian Federation Ministry of Science and Education contract 14.518.11.7046. The work was partly fulfilled during VSP visit to the University of Maryland, USA, where it was supported by the NASA grant NNX13AC46G.

## References

- [1] K. Greisen, *End to the cosmic ray spectrum?*, *Phys. Rev. Lett.* **16** (1966) 748
- [2] G.T. Zatsepin and V.A. Kuzmin, *Upper limit of the spectrum of cosmic rays*, *JETP Lett.* **4** (1966) 78
- [3] D. Allard, *Extragalactic propagation of ultrahigh energy cosmic rays*, *Astropart. Phys.* **39** (2012) 33
- [4] R. Aloisio, V. Berezhinsky, P. Blasi, *Ultra high energy cosmic rays: implications of Auger data for source spectra and chemical composition*, *JCAP* **10** (2013) 020
- [5] K. Kotera and A.V. Olinto, *The astrophysics of ultrahigh energy cosmic rays*, *Annu. Rev. Astron. Astrophys.* **49** (2011) 119
- [6] M. Lemoine, *Acceleration and propagation of ultrahigh energy cosmic rays*, *JPhCS* **409** (2012) 012007
- [7] P. Blasi, *Origin of very high and ultra-high energy cosmic rays*, *Comptes rendus-Physique* **15** (2014) 329
- [8] S.V. Troitsky, *Cosmic particles with energies above  $10^{19}$  eV: a brief review of results*, *Physics Uspekhi* **56** (2013) 304
- [9] A. Watson, *High-energy cosmic rays and the Greisen-Zatsepin-Kuzmin effect*, *Reports on Progress in Physics* **77** (2014) 036901
- [10] D. Allard, *Propagation of extragalactic ultra-high energy cosmic-ray nuclei: implications for the observed spectrum and composition*, *eprint arXiv:0906.3156v1* (2009)
- [11] V.S. Ptuskin, S.I. Rogovaya and V.N. Zirakashvili, *On ultra-high energy cosmic rays: origin in AGN jets and transport in expanding Universe*, *Adv. Space Res.* **51** (2013) 315

- [12] V.S. Berezhinsky, A. Gazizov and S. Grigorieva, *On astrophysical solution to ultrahigh energy cosmic rays*, *Phys. Rev. D* **74** (2006) 3005
- [13] R. Aloisio, V. Berezhinsky, S. Grigiriev, *Analytical calculations of the spectra of ultra-high energy cosmic ray nuclei. I. The case of CMB radiation*, *Astroparticle Physics* **41** (20013) 73
- [14] The Pierre Auger collaboration, *Bounds on the density of sources of ultra-high energy cosmic rays from the Pierre Auger Observatory*, *JCAP* **05** (2013) 009
- [15] D. Hooper, S. Sarkar, A.M. Taylor, *The intergalactic propagation of ultra-high energy cosmic ray nuclei: an analytic approach*, *Phys Rev D* **77** (2008) 3007
- [16] A.M. Taylor, M. Ahlers, F.A. Aharonian, *Need for a local source of ultrahigh-energy cosmic ray nuclei*, *Phys Rev D* **84** (2011) 5007
- [17] V. Berezhinsky, A. Gazizov, M. Kachelries, *Second dip as a signature of ultrahigh energy proton interactions with Cosmic Microwave Background radiation*, *Phys Rev Letters* **97** (2006) 1101
- [18] V.F. Turchin, V.P. Kozlov and M.S. Malkevich, *Reviews of topical problems: the use of mathematical-statistics methods in the solution of incorrectly posed problems*, *Sov. Phys. Uspekhi* **13** (1971) 681
- [19] A.N. Tikhonov and V.Y. Arsenin, *Solutions of Ill-Posed Problems*. New York: Winston, 1977
- [20] L.B. Lucy, *Optimum strategies for inverse problems in statistical astronomy*, *Astron. Astrophys.* **289** (1994) 983
- [21] H. Sagawa for the Telescope Array Collaboration, *Highlights from the Telescope Array Experiment 33rd International Cosmic Ray Conference, Rio de Janeiro, 2013*, in press
- [22] A. Letessier-Selvon for the Pierre Auger Collaboration, *Highlights from the Pierre Auger Observatory 33rd International Cosmic Ray Conference, Rio de Janeiro, 2013*, in press eprint *arXiv:1310.2118v1* (2013)
- [23] A.J. Barger, L.L. Cowie, Mushotzky et. al. *The cosmic evolution of hard X-ray-selected Active Galactic Nuclei*, *Astron J* **129** (2005) 578
- [24] R. Aloisio, V.S. Berezhinsky, *Anti-GZK effect in UHECR spectrum*, *ApJ* **625** (2005) 249
- [25] K. Kotera, M. Lemoine, *Inhomogeneous extragalactic magnetic fields and the second knee in the cosmic ray spectrum*, *Phys Rev D* **77** (2008) 3005
- [26] H. Takami, K. Sato, *Astropart Phys*, **30** (2009) 306
- [27] D. Allard, N.G. Busca, G. Decerprit, A.V. Olinto, E. Parizot, *Implications of the cosmic ray spectrum for the mass composition at the highest energies*, *J. Cosmol. Astropart. Phys.* **10** (2008) 33
- [28] R. Aloisio, V. Berezhinsky, A. Gazizov, *Ultra high energy cosmic rays: the disappointing model* *Astropart. Phys.* **34** (2011) 620